JOURNAL OF SOLID STATE CHEMISTRY **127,** 145–150 (1996)
ARTICLE NO. 0370

Synthesis and Structure of a Chain Aluminophosphate Filled with $[NH_4]^+$ and $[H_3NCH_2CH_2NH_3]^{2+}$ Cations[1]

Qiuming Gao, Jiesheng Chen, Shougui Li, and Ruren Xu

Key Laboratory of Inorganic Hydrothermal Synthesis, Department of Chemistry, Jilin University, Changchun 130023, China

John Meurig Thomas

Davy Faraday Research Laboratory, The Royal Institution of Great Britain, 21 Albemarle Street, London W1X 4BS, United Kingdom

and

Mark Light and Michael B. Hursthouse

Department of Chemistry, University of Wales Cardiff, P.O. Box 912, Cardiff, CF1 3TB, United Kingdom

Received January 18, 1996; in revised form August 9, 1996; accepted August 14, 1996

The compound $[AlP_2O_8]^{3-}[NH_3CH_2CH_2NH_3]^{2+}[NH_4]^+$ (designated ALPO-enA, where enA stands for ethylenediammonium and ammonium cations) has been synthesized from the nonaqueous system H_3PO_4–Al(O*i*-Pr)$_3$–$NH_2CH_2CH_2NH_2$–$HOCH_2CH_2OH$–H_2O. The structure of the compound has been characterized by single crystal X-ray diffraction to be orthorhombic with space group *Pccn* and unit cell dimensions $a = 8.0330(10)$, $b = 16.989(2)$, $c = 8.740(2)$ Å and $Z = 4$. The final R_1 and wR_2 values were 0.0309 and 0.0706. The structure consists of macroanionic $[AlP_2O_8]^{3-}$ chains built up from AlO_4 and PO_4 tetrahedra, in which all AlO_4 vertices are shared but each PO_4 has two terminal P–O groups. The cations which balance the negative charges of the chains are $[NH_3CH_2CH_2NH_3]^{2+}$ and $[NH_4]^+$, the latter being believed to arise from the fragmentation of the former during crystallization. Additional characterization of the compound by powder XRD, SEM, IR spectroscopy, inductively coupled plasma analysis (ICP), TGA, and DTA are also described.

INTRODUCTION

Three-dimensional microporous aluminophosphates ($AlPO_4$-*n* with *n* representing a particular structure type) were discovered by Wilson and others (1–3) in the 1980s. Since then, much effort has been directed toward synthesis and structural characterization of novel but $AlPO_4$-*n* related materials. Structurally, most $AlPO_4$-*n* phases are exclusively composed of PO_4 and AlO_4 primary building units although a few contain AlO_5 and AlO_6 units (4, 5). Recently, several layered aluminophosphates (6–8) have been synthesized with various P : Al ratios (e.g., 3 : 2 (6) and 4 : 3 (7, 8)) and a range of ring sizes within the layer. Stacking of the rings can result in microporosity in some of these materials (8). A 1-dimensional chain aluminophosphate with P : Al ratio of 2 : 1 has also been found (9), and contains P=O $\cdots$ HO–P internal hydrogen bonds. Here we report another chain aluminophosphate $[AlP_2O_8]^{3-}$ $[H_3NCH_2CH_2NH_3]^{2+}[NH_4]^+$ (designated ALPO-enA), during the crystallization of which the templating agent (ethylenediamine) is fragmented, leading to the coexistence of $[H_3NCH_2CH_2NH_3]^{2+}$ and $[NH_4]^+$ between the inorganic $[AlP_2O_8]^{3-}$ chains of the compound. There are no P=O $\cdots$ HO–P internal hydrogen-bonds in the present chain aluminophosphate.

EXPERIMENTAL

Synthesis of $[AlP_2O_8]^{3-}[H_3NCH_2CH_2NH_3]^{2+}[NH_4]^+$ (*ALPO-enA*)

ALPO-enA was synthesized from a mixture of H_3PO_4–(*i*-PrO)$_3$Al–ethylenediamine–ethylene glycol–water. (*i*-PrO)$_3$Al was first slurried with the solvent ethylene glycol (EG), then ethylenediamine (en) was added with stirring. Phosphoric acid was slowly added to the mixture until the

[1] See NAPS document No. 05354 for 8 pages of supplementary material Order from ASIS/NAPS, Microfiche Publications, P.O. Box 3513, Grand Central Station, New York, NY 10163. Remit in advance $4.00 for microfiche copy or for photocopy, $7.75 up to 20 pages plus $.30 for each additional page. All orders must be prepaid. Institutions and Organizations may order by purchase order. However, there is a billing and handling charge for this service of $15. Foreign orders add $4.50 for postage and handling, for the first 20 pages, and $1.00 for additional 10 pages of material, $1.50 for postage of any microfiche orders.

0022-4596/96 $18.00

TABLE 1
Crystal Data and Structure Refinement for ALPO-enA

Empricial formula	$C_2H_{14}N_3AlP_2O_8$
Formula weight	297.08
Collection temperature (K)	293(2)
Wavelength (Å)	0.71069
Crystal system	Orthorhombic
Space group	*Pccn*
a (Å)	8.0330(10)
b (Å)	16.989(2)
c (Å)	8.740(2)
alpha (°)	90.000
beta (°)	90.000
gamma (°)	90.000
Volume (Å^3)	1192.8(3)
Z	4
Density (calculated) (Mg m^{-3})	1.654
Absorption coefficient (mm^{-1})	0.469
F(000)	616
Crystal size (mm)	0.1 × 0.2 × 0.15
Theta range for data collection	2.40 to 25.08°
Index ranges	$-8 \leqq h \leqq 8$, $-19 \leqq k \leqq 19$, $-8 \leqq l \leqq 10$
Reflections collected	4498
Independent reflections	963 [R(int) = 0.0699]
Refinement method	Full-matrix least-squares on F^2
Data/restrains/parameters	963/0/102
Goodness of fit on F^2	0.902
Final R indices [I > 2 sigma(I)]	$R1$ = 0.0309, w$R2$ = 0.0706
R indices (all data)	$R1$ = 0.0544, w$R2$ = 0.0729
Largest difference peak and hole (e Å^{-3})	0.362 and −0.313

$R1 = \Sigma(\Delta F)/\Sigma(Fo)$.
$wR2 = [\Sigma[w(Fo^2 - Fc^2)^2])/\Sigma[w(F_0^2)^2]]^{1/2}$.
$w = 1/\sigma^2[Fo^2]$.

molar composition $1.0Al_2O_3 : 3.0P_2O_5 : 5.0$en: 90.0EG : 12.3 H_2O was reached. The final reaction mixture was stirred until a homogenous gel was formed. The gel was sealed in a Teflon-lined stainless-steel autoclave and heated under autogenous pressure at 180°C for 20 days. The colorless crystalline product was filtered, washed with distilled water, and dried at ambient temperature.

Characterization

X-ray powder diffraction (XRD) data were collected on a Rigaku D/MAX III diffractometer with Ni-filtered Cu$K\alpha$ radiation (λ = 1.5418 Å). Element analyses were performed on a Perkin–Elmer 240C element analyzer. Inductively coupled plasma analysis (ICP) was carried out on a Jarrell–Ash 800 Mark-II ICP instrument. The scanning electron micrographs (SEM) were taken with a Hitachi X-650B electron microscope. The IR spectra were recorded on a Nicolet 5DX FTIR spectrometer using *K*Br pellets. A Perkin–Elmer DTA 1700 differential thermal analyzer was used to obtain the differential thermal analysis (DTA) and a Perkin–Elmer TGA 7 thermogravimetric analyzer was used to obtain the thermogravimetric analysis (TGA) curves in an atmospheric environment. The heating rate was 20°C min^{-1}.

TABLE 2
Atomic Coordinates (×10^4) and Equivalent Isotropic Displacement Parameters (A^2 × 10^3) for Nonhydrogen Atoms, and Isotropic Displacement Parameters for Hydrogen Hydrogen Atoms for ALPO-enA

	x	*y*	*z*	*U*(eq/iso)
P(1)	613(1)	1478(1)	1378(1)	17(1)
Al(1)	2500	2500	−1137(1)	15(1)
O(1)	1294(2)	663(1)	1509(2)	34(1)
O(2)	1322(3)	1875(1)	−44(2)	48(1)
O(3)	1127(3)	1976(1)	2767(2)	42(1)
O(4)	−1255(2)	1501(1)	1294(2)	31(1)
N(1)	−2500	2500	3810(5)	29(1)
N(2)	−2858(3)	101(2)	855(3)	23(1)
C(1)	−4483(4)	353(2)	214(4)	26(1)
H(1A)	−5027(37)	683(21)	993(35)	45(9)
H(1B)	−4249(32)	701(18)	−765(33)	34(8)
H(5A)	−1858(45)	2148(21)	3257(36)	60(12)
H(5B)	−1947(45)	2820(21)	4330(37)	57(12)
H(6A)	−2290(36)	508(20)	1074(28)	29(9)
H(6B)	1953(35)	201(17)	3232(32)	35(9)
H(6C)	2274(41)	231(19)	−226(37)	56(11)

Note. *U*(eq) is defined as one third of the trace of the orthogonalized. U_{ij} tensor.

Structure Determination

The crystal selected for X-ray work had dimensions of 200 × 150 × 100 μm and was mounted with Araldite on a glass fiber. Cell dimensions and intensity data were recorded at 293 K, as previously described (10) using a FAST TV area detector diffractometer mounted at the window of a rotating anode operating at 50 KV, 50 mA with a molybdenum anode (λMo$K\alpha$) = 0.71069 Å). The

TABLE 3
Bond Lengths (Å) for ALPO-enA

P(1)–O(1)	1.493(2)	P(1)–O(2)	1.525(2)
P(1)–O(3)	1.537(2)	P(1)–O(4)	1.503(2)
Al(1)–O(2)	1.713(2)	Al(1)–O(2)#3	1.713(2)
Al(1)–O(3)#1	1.711(2)	Al(1)–O(3)#2	1.711(2)
N(1)–H(5A)	0.93(4)	N(2)–H(6A)	0.85(3)
N(1)–H(5B)	0.84(3)	C(1)–H(1A)	0.99(3)
N(2)–C(1)	1.483(4)	N(2)–H(6C)	0.89(4)
N(2)–H(6B)	0.95(3)	C(1)–H(1B)	1.06(3)
C(1)–C(1)#5	1.506(6)		

Note. Symmetry transformations used to generate equivalent atoms: #1 x, $-y + 0.5$, $z - 0.5$; #2 $-x + 0.5$, y, $z - 0.5$; #3 $-x + 0.5$, $-y + 0.5$, z; #4 x, $-y + 0.5$, $z + 0.5$; #5 $-x - 1$, $-y$, $-z$.

TABLE 4
Bond Angles (°) for ALPO-enA

O(1)–P(1)–O(4)	113.24(12)	O(1)–P(1)–O(2)	109.68(12)
O(4)–P(1)–O(2)	108.74(13)	O(1)–P(1)–O(3)	110.57(12)
O(4)–P(1)–O(3)	106.97(12)	O(2)–P(1)–O(3)	107.44(12)
O(3)#1–Al(1)–O(3)#2	111.9(2)	O(3)#1–Al(1)–O(2)#3	110.22(11)
O(3)#2–Al(1)–O(2)#3	106.17(11)	O(3)#1–Al(1)–O(2)	106.17(11)
O(3)#2–Al(1)–O(2)	110.22(11)	O(2)#3–Al(1)–O(2)	112.2(2)
P(1)–O(2)–Al(1)	159.3(2)	P(1)–O(3)–Al(1)#4	154.4(2)
H(5A)–N(1)–H(5B)	114(4)	C(1)–N(2)–H(6A)	109(2)
N(2)–C(1)–C(1)#5	110.4(3)	N(2)–C(1)–H(1A)	107(2)
C(1)#5–C(1)–H(1A)	112(2)	N(2)–C(1)–H(1B)	108(2)
C(1)#5–C(1)–H(1B)	110(2)	H(1A)–C(1)–H(1B)	109(2)
H(6A)–N(2)–H(6B)	108.2(2)	H(6A)–N(2)–H(6C)	112.8(3)
H(6B)–N(2)–H(6C)	103.1(3)	C(1)–N(2)–H(6C)	111.4(4)

Note. Symmetry transformations used to generate equivalent atoms: #1 x, $-y + 0.5$, $z - 0.5$; #2 $-x + 0.5$, y, $z - 0.5$; #3 $-x + 0.5$, $-y + 0.5$, z; #4 x, $-y + 0.5$, $z + 0.5$; #5 $-x - 1$, $-y$, $-z$.

crystal-to-detector distance was 50 mm and the detector 2θ swing angle was 20°. Slightly more than one hemisphere of data were recorded. Following normal data processing, the space group was determined as *Pccn* from analysis of the systematically absent reflections. The structure was solved via direct methods (11) and refined by full matrix least squares (12). A correction for absorption was made using the program DIFABS (13), the maximum, minimum, and average correction factors were 1.097, 0.894, and 1.010. Nonhydrogen atoms were refined anisotropically; hydrogen atoms were located in a difference map and were successfully refined with individual isotropic displacement factor coefficients. Refinement was based on F^2, and involved a total of 102 parameters. Crystal data, details of data collection, and refinement are given in Table 1.

RESULTS AND DISCUSSION

Description of the Structure

The atomic coordinates, bond distances and bond angles are listed in Table 2, Table 3, and Table 4, respectively.

ALPO-enA consists of macroanionic chains (empirical formula $[AlP_2O_8]^{3-}$), separated by $[NH_4]^+$ and $[H_3NCH_2CH_2NH_3]^{2+}$ cations. In the asymmetric unit there is one crystallographically independent P atom and one special position Al atom. Figures 1, 2a, and 2b show the crystal structure as viewed in the *a* and *c* directions. Each Al atom is tetrahedrally coordinated by four O atoms with Al–O contacts varying between 1.711 and 1.713 Å and O–Al–O angles lying between 106.2 and 112.2°. These values are in good agreement with those found in the mineral berlinite (14). Each P atom is also tetrahedrally coordinated to four O atoms. Two of these atoms are bonded to aluminum atoms with P–O bond lengths of 1.525 and 1.537 Å. The remaining P–O bonds (i.e., P(1)–O(1) and P(1)–O(4) of lengths 1.493 and 1.503 Å, respectively) both clearly have multiple bond character, and are comparable with those in, for example, $H_3PO_4 \cdot 0.5H_2O$ (1.485 and 1.495 Å, respectively) (15). No P–OH bond is present, the bond length of which should be between 1.55–1.56 Å as found in $H_3PO_4 \cdot 0.5H_2O$ and α-zirconium phosphate (16). The multiple-bond nature of the P–O bonds is also reflected in the O ··· P ··· O angle (113.2°) which is greater than the O–P ··· O and O–P–O angles (107.0(1)–110.6(1)°), as expected on the basis of elementary VSEPR (valence shell electron pair repulsion) theory.

This structure is different from that of $[AlP_2O_8H_2]^-$

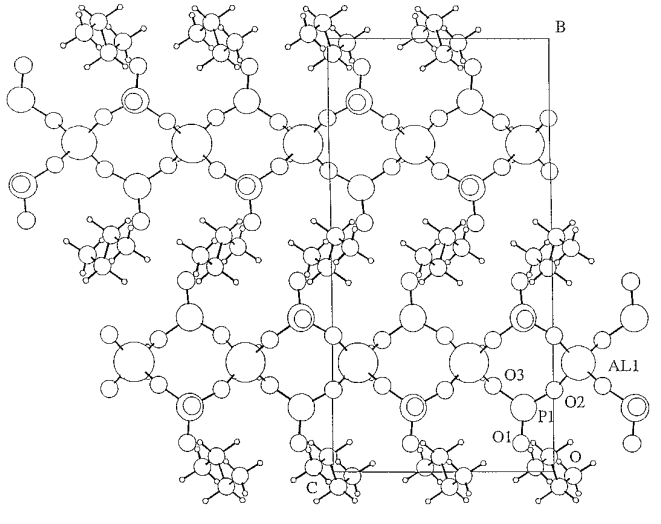

FIG. 1. SNOOPI (31) drawing of the structure of ALPO-enA viewed down the *a* axis. O(4) is situated directly below P(1) and the NH_4 group directly below Al(1).

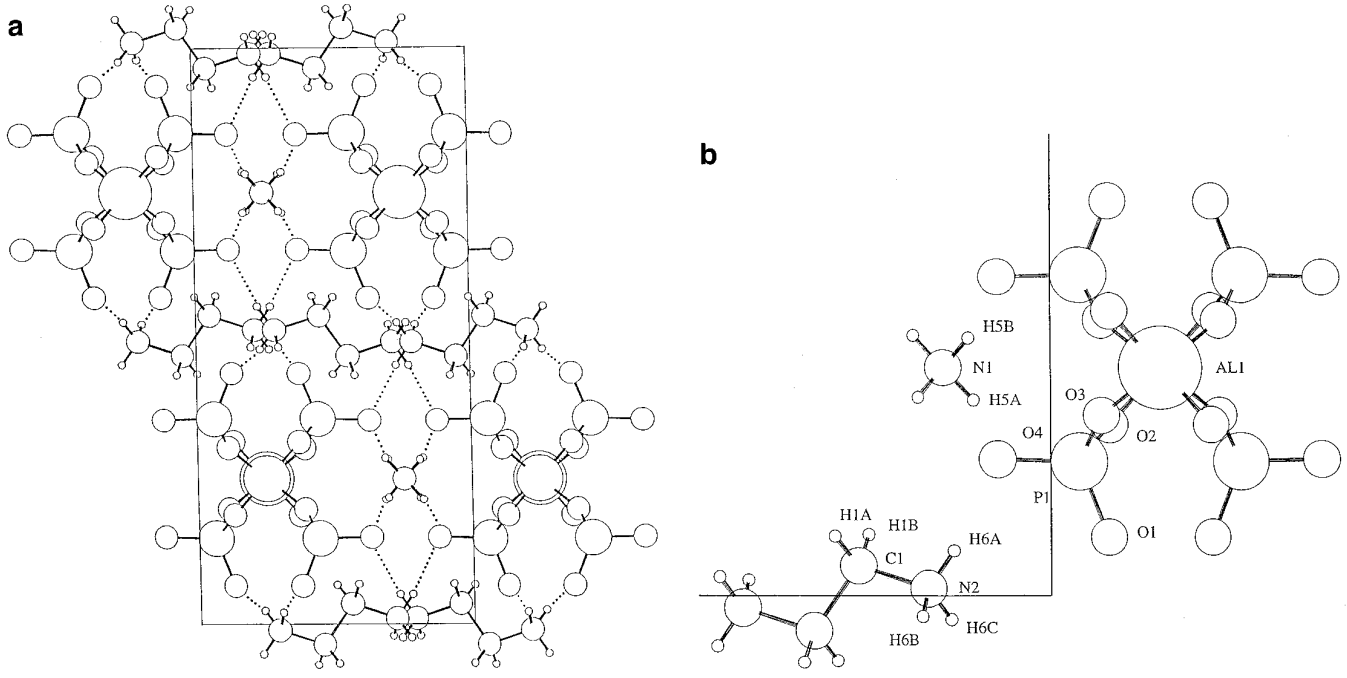

FIG. 2. (a) SNOOPI (31) drawing of the structure of ALPO-enA viewed down the *c* axis. Hydrogen bonds are dotted. (b) SNOOPI (31) drawing of part of the structure of ALPO-enA viewed down the *c* axis and showing the labeling of the asymmetric unit.

$[Et_3NH]^+$, (9) in which two of the PO_4 vertices are linked to adjacent AlO_4 units, and of the remaining two, one is a P=O bond and the other a P–OH group. The latter two types of function form P=O ··· HO–P hydrogen bonds within the inorganic chain. It follows that the number of the hydrogen atoms on each chain unit depends on the bulkiness of the template: the bulkier the template, the more hydrogen atoms on the inorganic chain. Ethylenediammonium and ammonium cations are smaller than triethylammonium, and as a result, two cations instead of one for each $[AlP_2O_8]^{3-}$ unit are present between the inorganic chains. The cations are held in place by single hydrogen bonds between each of the hydrogens of the R–NH_3^+ and NH_4^+ groups and the terminal oxygens O(1) and O(4) of the framework. These are shown in Table 5 (17) and Fig. 2a.

It is unusual that the occluded cations are of two types, $[NH_4]^+$ and $[H_3NCH_2CH_2NH_3]^{2+}$, whereas the template used in the reaction mixture is ethylenediamine only. Obviously, the $[NH_4]^+$ must have arisen from the fragmentation of ethylenediammonium at a pH as low as about 3.5 in the reaction mixture. Template fragmentation were also observed previously (18, 19).

Characterization of ALPO-enA

The crystals appear as long rods and the crystal size is considerably homogenous (ca 200 × 150 × 100 μm). ICP analysis indicates that ALPO-enA contains 8.9 wt% Al and 20.9 wt% P, in agreement with the result of EDAX (ca molar ratio Al : P = 0.5). Element analysis indicates that the C, H, and N contents are 7.28, 4.27, and 11.40 wt%, respectively, corresponding to an empirical molar ratio C : H : N = 1.00 : 7.05 : 1.34. The analysis results are in accordance with the formula $[AlP_2O_8]^{3-}[H_3NCH_2CH_2NH_3]^{2+}[NH_4]^+$.

ALPO-enA exhibits an X-ray powder diffraction pattern (Fig. 3) different from that of $[AlP_2O_8H_2]^-[Et_3NH]^+$ though the inorganic chains for these two compositions are similar. On the basis of the framework vibration model for microporous aluminophosphates, the absorption bands for ALPO-enA (Fig. 4) are assigned as follows (21–23): 1159, 1117, and 1033 cm^{-1} are associated with the asymmet-

TABLE 5
Possible Hydrogen Bonds

Interaction	*S*	*d*1 (Å)	*d*2 (Å)	*d*3 (Å)	Angle (°)
N(1)–H(5A) ··· O(4)		0.950	2.087	2.953	150.83
N(1)–H(5B) ··· O(4)	1	0.880	2.093	2.929	158.45
N(2)–H(6A) ··· O(4)		0.866	1.875	2.731	169.12
N(2)–H(6B) ··· O(1)	2	0.955	1.790	2.729	167.10
N(2)–H(6C) ··· O(1)	3	0.902	1.870	2.743	162.55

Note. S, Symmetry operator; 1, x, $-y + 0.5$, $z + 0.5$; 2, $x - 0.5$, $-y$, $-z + 0.5$; 3, $-x$, $-y$, $-z$. *d*1, N–H; *d*2, H ··· O; *d*3, N ··· O; angle N–H ··· O.

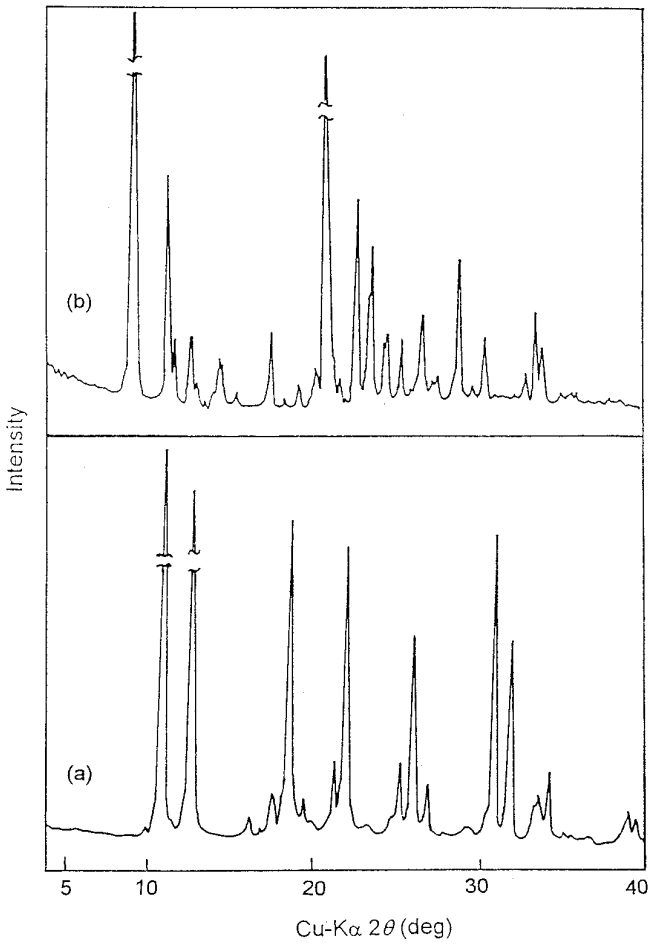

FIG. 3. X-ray powder diffraction patterns for (a) ALPO-enA and (b) $[AlP_2O_8H_2]^-[Et_3NH]^+$.

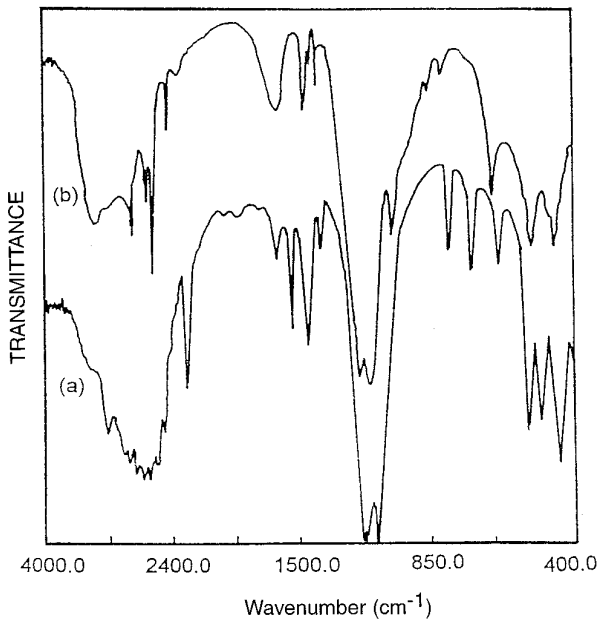

FIG. 4. IR Spectra of (a) ALPO-enA and (b) $[AlP_2O_8H_2]^-[Et_3NH]^+$.

density difference between these two compounds based on the structural analysis: for ALPO-enA, $d = 1.654$ mg/cm^3; whereas for $[AlP_2O_8H_2]^-[Et_3NH]^+$, (9) $d = 1.548$ mg/cm^3. From the derivation of the TGA curve, we can see that there are two weight losses for ALPO-enA: the loss of $[NH_4]^+$ is at ca 230°C and that of the ethylenediammonium ions occurs at ca 350°C, suggesting that the decomposition of ethylenediammonium is more difficult than that of the ammonium cations. The weight loss of $[NH_4]^+$ is ca 6.0 wt% and that of $[H_3NCH_2CH_2NH_3]^{2+}$ is ca 21.7 wt%

ric stretching vibrations of PO_4 units whereas those at 794 and 723 cm^{-1} correspond to symmetric stretching vibrations of PO_4 groups; the bands at 639, 548, 513, and 449 cm^{-1} are related to bending vibrations of PO_4 groups or the vibration modes of the 4-membered rings of the aluminophosphate chain. Compared with $[AlP_2O_8H_2]^-[Et_3NH]^+$, the stretching vibrations of PO_4 for ALPO-enA are shifted toward lower frequency, indicating that the presence of the internal P=O $\cdots$ HO–P hydrogen bonds plays a key role in determining the strength of the P–O bonds. Bands arising from (24–26) the template cations $[NH_3CH_2CH_2NH_3]^{2+}$ and $[NH_4]^+$ are also seen. The bands at 1652 and 1553 cm^{-1} may be due to δ_{N-H} (in plane) of the -NH_3^+ or NH_4^+, and the bands at 1448 and 1370 cm^{-1} are assigned to asymmetric stretching vibration of -CH_2-. The broad band at 2756 cm^{-1} is due to ν_{N-H}.

The TGA curve (Fig. 5) shows that the weight loss of ALPO-enA is about 27.7 wt%, less than that (36.6 wt%) for $[AlP_2O_8H_2]^-[Et_3NH]^+$. This is also reflected by the

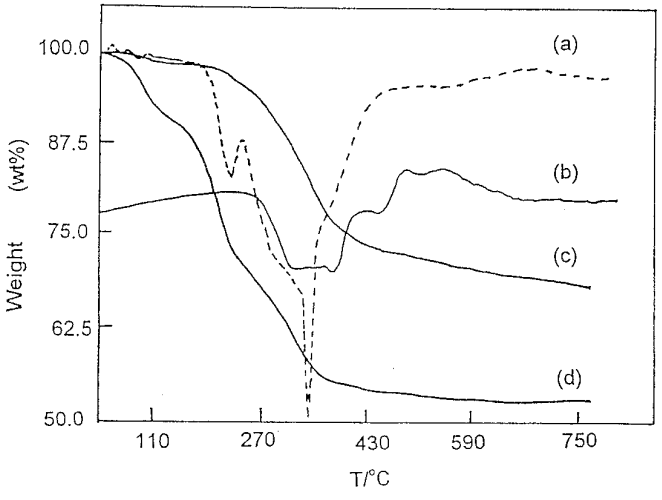

FIG. 5. Thermal analysis curves: (a) derivation of TGA, (b) DTA, (c) TGA curve for ALPO-enA, and (d) TGA for $[AlP_2O_8H_2]^-[Et_3NH]^+$ as a comparison.

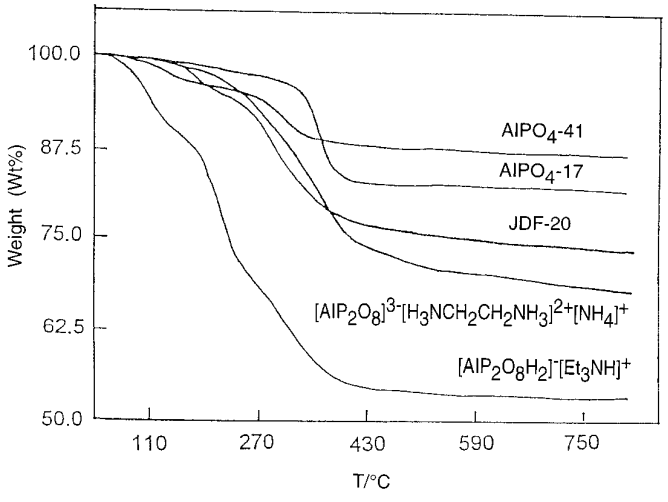

FIG. 6. TGA curves for $AlPO_4$-41, $AlPO_4$-17, JDF-20, ALPO-enA, and $[AlP_2O_8H_2]^-[Et_3NH]^+$.

in agreement with the formula $[AlP_2O_8H_2]^{3-}[H_3NCH_2CH_2NH_3]^{2+}[NH_4]^+$. The total weight losses for both (Fig. 6) ALPO-enA and $[AlP_2O_8H_2]^-[Et_3NH]^+$ are larger than that for 3-dimensional microporous aluminophosphates, such as $AlPO_4$-41 with a 1-dimensional medium-pore framework (27), $AlPO_4$-17 (28) with a cage-containing framework and JDF-20 (29, 30), an aluminophosphate possessing 20-member ring channels. It can be concluded that 1-dimensional chain aluminophosphates have larger void contents than 3-dimensional materials.

CONCLUSIONS

The successful synthesis of the 1-dimensional chain aluminophosphate $[AlP_2O_8]^{3-}[H_3NCH_2CH_2NH_3]^{2+}[NH_4]^+$ further reveals the advantage of alcoholic systems for the formation of aluminophosphates with low Al/P ratios. With variation of templating agent and crystallization conditions, new compounds with novel structural features are obtainable.

ACKNOWLEDGMENTS

We thank the National Natural Science Foundation (China), the Ph.D. Studentship Foundation (China), and the EPSRC (U.K.) for financial support.

REFERENCES

1. S. T. Wilson, B. M. Lok, and E. M. Flanigen, U.S. Patent 4 310 440 (1982).
2. E. M. Flanigen, B. M. Lok, R. L. Patton, and S. T. Wilsion, *Pure Appl. Chem.* **58,** 1351 (1986).
3. M. E. Davis, C. Saldarriaga, C. Montes, and C. Crowder, *Nature* **331,** 698 (1988).
4. J. V. Smith, *Chem. Rev.* **88,** 149 (1988).
5. J. M. Bennett, J. M. Cohen, G. Artiol, J. J. Pluth, and J. V. Smith, *Inorg. Chem.* **24,** 188 (1985).
6. A. M. Chippindale, A. V. Powell, L. M. Bull, R. H. Jones, A. K. Cheetham, J. M. Thomas, and R. Xu, *J. Solid State Chem.* **96,** 199 (1992).
7. R. H. Jones, J. M. Thomas, R. Xu, Q. Huo, A. K. Cheetham, and A. V. Powell, *J. Chem. Soc. Chem. Commun.* 1266, (1991).
8. J. M. Thomas, R. H. Jones, R. Xu, J. Chen, A. M. Chippindale, S. Natarajan, and A. K. Cheetham, *J. Chem. Soc. Chem. Commun.* 929, (1992).
9. R. H. Jones, J. M. Thomas, R. Xu, Q. Huo, Y. Xu, A. K. Cheetham, and D. Bieber, *J. Chem. Soc. Chem. Commun.* 1170, (1990).
10. A. A. Danopoulos, G. Wilkinson, B. Hussain-Bates, and M. B. Hursthouse, *J. Chem. Soc. Dalton Trans.* 1855, (1991).
11. G. M. Sheldrick, "SHELXS-86," *Acta Crystallogr. A* **46,** 467 (1990).
12. G. M. Sheldrick, "SHELXL-93," Program for Crystal Structure Refinement, University of Göttingen, Germany (1993).
13. N. P. C. Walker and C. Stuart, *Acta Crystallogr. A* ***39,*** 158 (1983), (adapted for FAST geometry by A. Karaulov, University of Wales, Cardiff, 1991).
14. D. Schwarzenbach, *Z. Kristallogr* **123,** 161 (1966).
15. B. Dickens, E. Prince, L. W. Schroeder, and T. H. Jordan, *Acta Crystallogr. Struct. Crystallogr. Cryst. Chem. B* **30,** 1470 (1974).
16. J. M. Troup and A. Clearfield, *Inorg. Chem.* **16,** 3311 (1977).
17. M. Nardelli, Parst, Program for Calculating Molecular Parameters, *Comp. Chem.* **7,** 95 (1983).
18. A. M. Chippindale, S. Natarajan, and J. M. Thomas, *J. Solid State Chem.* **111,** 18 (1994).
19. J. M. Bennett, W. J. Dytrych, J. J. Pluth, J. W. Richardson, and J. V. Smith, *Zeolites* **6,** 349 (1986).
20. Y. Xu, X. Jiang, X. Meng, and R. Xu, *Acta Petrol. Sin.* **3,** 101 (1987).
21. R. A. van Nordstrand, D. S. Santilli, and S. I. Zones, *ACS Symp. Ser.* **368,** 236 (1988).
22. M. E. Davis, P. E. Hathaway, C. Montes, and J. M. Gares, *Stud. Surf. Sci. Catal.* **49,** 199 (1989).
23. A. Stein, B. Wehrle, and M. Jonsen, *Zeolites* **13,** 291 (1993).
24. M. E. Davis, C. Montes, P. E. Hathaway, J. P. Arhancet, D. L. Hasha, and J. Garces, *J. Am. Chem. Soc.* **111,** 3919 (1989).
25. Q. Jin *et al.* (Eds.), "Instrument Analysis." Jilin Univ. Press, Vol. 130, 1988.
26. "Structural Methods in Inorganic Chemistry." Blackwell Sci. Oxford, Vol. 164, 1987.
27. Q. Gao, J. Chen, S. Li, and R. Xu, in preparation.
28. Q. Gao, S. Li, and R. Xu, *J. Chem. Soc. Chem. Commun.* 1465, (1994).
29. Q. Huo, R. Xu, S. Li, Z. Ma, J. M. Thomas, R. H. Jones, and A. M. Chippindale, *J. Chem. Soc. Chem. Commun.* 875, (1992).
30. R. H. Jones, J. M. Thomas, J. Chen, R. Xu, Q. Huo, S. Li, Z. Ma, and A. M. Chippindale, *J. Solid State Chem.* **102,** 204 (1993).
31. K. Davies, "SNOOPI Program for Crystal Structure Drawing," University of Oxford, U.K., (1983).